Supporting Information

AIE-active TPA modified Schiff base for successive sensing of Cu^{2+} and His via on-off-on method and its application in bioimaging

Dan Wang,*[a] Tian-Fen Shao,[a] Wei-Hua Ding,[b] Shao-Jie Li,[a] Qi Yao,[a] Wei Cao,[c] Zheng Wang[a] and Yangmin Ma[a]

[a] *Key Laboratory of Chemical Additives for China National Light Industry, College of Chemistry and Chemical Engineering, Shaanxi University of Science & Technology, Xi'an 710021, People's Republic of China.*

[b] *Medical School, Institute of Reproductive Medicine, Nantong University, Nantong, Jiangsu 226001, People's Republic of China.*

[c] *Scientific Instrument Center, Shanxi University, Taiyuan 030006, People's Republic of China.*

Corresponding author:

E-mail address:

wangdan0919@163.com (D. Wang)

1. Materials and Apparatus

All reagents were purchased from Energy Chemical or Macklin Biochemical Co., Ltd., and were used directly as received. Tetrahydrofuran (THF) used for spectral determination was of HPLC grade, other reagents were of analytical grade. The solutions of metal ions were prepared from $Al(ClO_4)_3 \cdot 9H_2O$, $CaCl_2$, $Cd(ClO_4)_2 \cdot H_2O$, $Co(ClO_4)_2 \cdot 6H_2O$, $CrCl_3 \cdot 6H_2O$, $FeCl_3 \cdot 6H_2O$, KCl, LiCl, $MgCl_2 \cdot 6H_2O$, $Mn(ClO_4)_2 \cdot 6H_2O$, NaCl, $Ni(ClO_4)_2 \cdot 6H_2O$, $Zn(ClO_4)_2 \cdot 6H_2O$, $Pb(ClO_4)_2 \cdot 3H_2O$, $FeCl_2$, $HgCl_2$, $Hg_2(NO_3)_2 \cdot 2H_2O$, $Cu(Ac)_2$, $Cu(ClO_4)_2 \cdot 6H_2O$, $Cu(NO_3)_2 \cdot 3H_2O$ and $CuCl_2 \cdot 2H_2O$. ^{1}H NMR and ^{13}C NMR spectra were acquired on a Bruker Ascend 400 (400 MHz) spectrometer. FT-IR spectra were obtained on a Bruker INVENIO Fourier transform infrared spectrometer using KBr pellets. ESI-HRMS were acquired on a Thermo Fisher Q Exactive mass spectrometer with an ESI interface. Fluorescence spectra were measured by a Thermo Scientific Lumina fluorescence spectrophotometer, with a quartz cuvette (path length = 1 cm). UV-Vis absorption spectra were recorded on an UV-2600 spectrophotometer. pH values were determined on a PHS-3E pH meter. Dynamic light scattering (DLS) data were obtained using a Zetasizer Nano ZS90 laser particle size and zeta potential analyzer (Malvern). Scanning electron microscope (SEM) measurements were performed on a Hitachi SU8100 SEM. Confocal fluorescence imaging was carried out on a Leica TCS SP2 Laser Confocal Microscope.

2. Preparation of compounds 2 and 3

N-(4-Nitrophenyl)-N-N-diphenylamine (2) and N-(4-aminophenyl)-N,N-diphenylamine (3) were prepared according to the reported literature[1, 2]. As shown in Scheme S1, compound 2 was synthesized by the reaction of diphenylamine with 4-fluoronitrobenzene in the presence of sodium hydride. The brown crude product was recrystallized in isopropanol to give pure compound 2 in a yield of 85% (1.2338 g). ^{1}H NMR (400 MHz, DMSO-d_6) δ 8.10 (d, J = 8.0 Hz, 2H), 7.49 (t, J = 8.0 Hz, 4H), 7.31 (m, 6H), 6.84 (d, J = 8.0 Hz, 2H) ppm. Compound 3 was synthesized by Pd/C-catalyzed reduction of compound 2. The raw product was recrystallized in ethanol to give pure compound 3 in a yield of 91% (0.2369 g). ^{1}H NMR (400 MHz, DMSO-d_6) δ 7.23 (t, J = 8.0 Hz, 4H), 6.92 (m, 6H), 6.83 (d, J = 8.0 Hz, 2H), 6.60 (d, J = 8.0 Hz, 2H), 5.07 (s, 2H) ppm. The ^{1}H NMR data of compounds 2 and 3 are in agreement the published data[1, 2].

3. Theoretical calculation methods

All calculations were carried out with the Gaussian 09 software[3]. The PBE0 functional[4] and the def2-SVP basis sets[5, 6] were adopted for geometry optimization calculations. The DFT-D3 with BJ-damping[7] was applied to correct the weak interaction to improve the calculation accuracy. The SMD implicit solvation model[8] was used to account for the solvation effect of water. Orbital energy level analysis was performed by Multiwfn software[9]. The visualization of the orbitals for **HL** and **CuL_2** complex were achieved using VMD[10] software. The excited states are calculated with linear response time-dependent DFT (TD-DFT) at the optimized ground state geometry. TD-DFT calculation was performed with PBE0 functional and the TZVP basis set[11, 12].

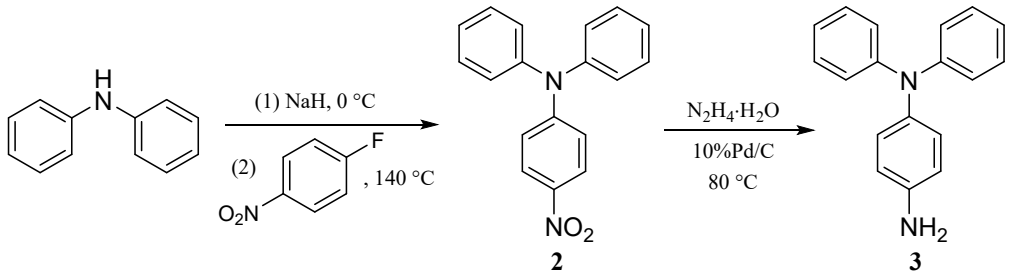

Scheme S1 The synthetic route for compound 3.

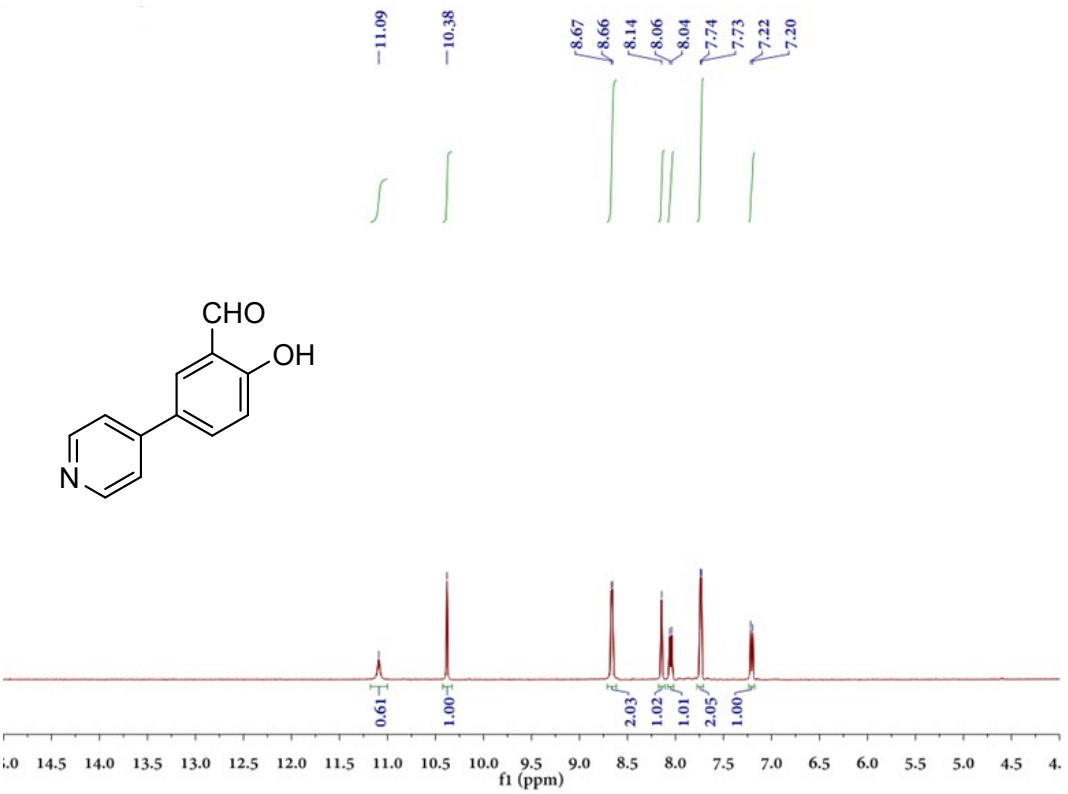

Fig. S1 ^{1}H NMR spectra of compound **1** in DMSO-d_6.

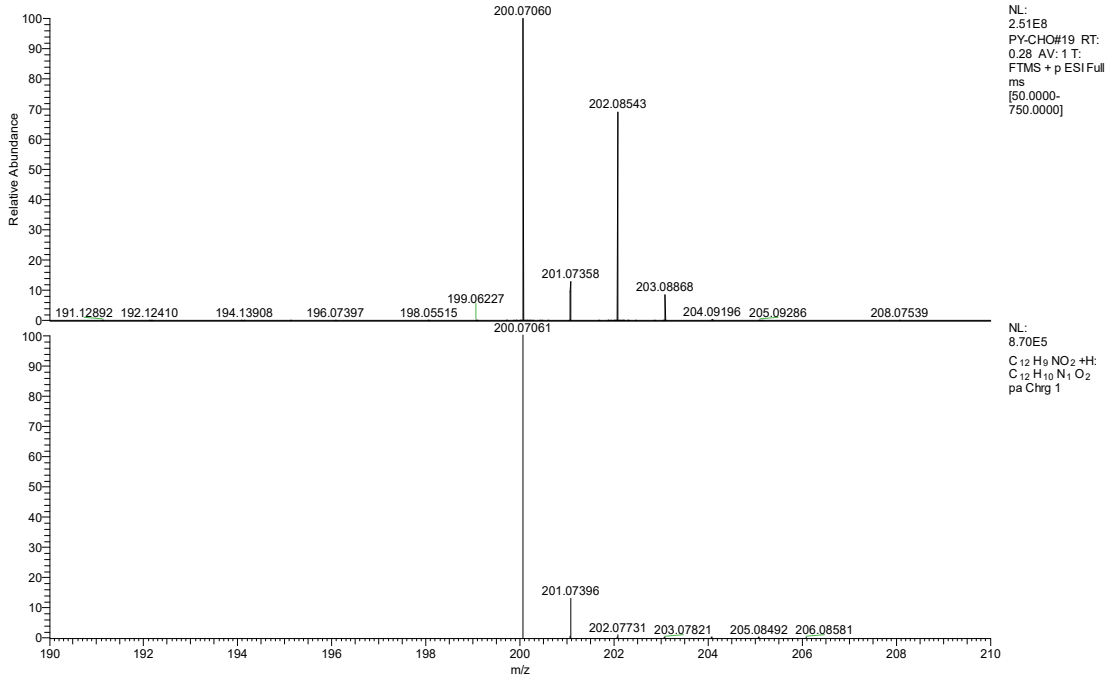

Fig. S2 (a) ESI-mass spectrum of compound **1** ($C_{12}H_9NO_2$). (b) The simulation pattern of $[H(C_{12}H_9NO_2)]^+$.

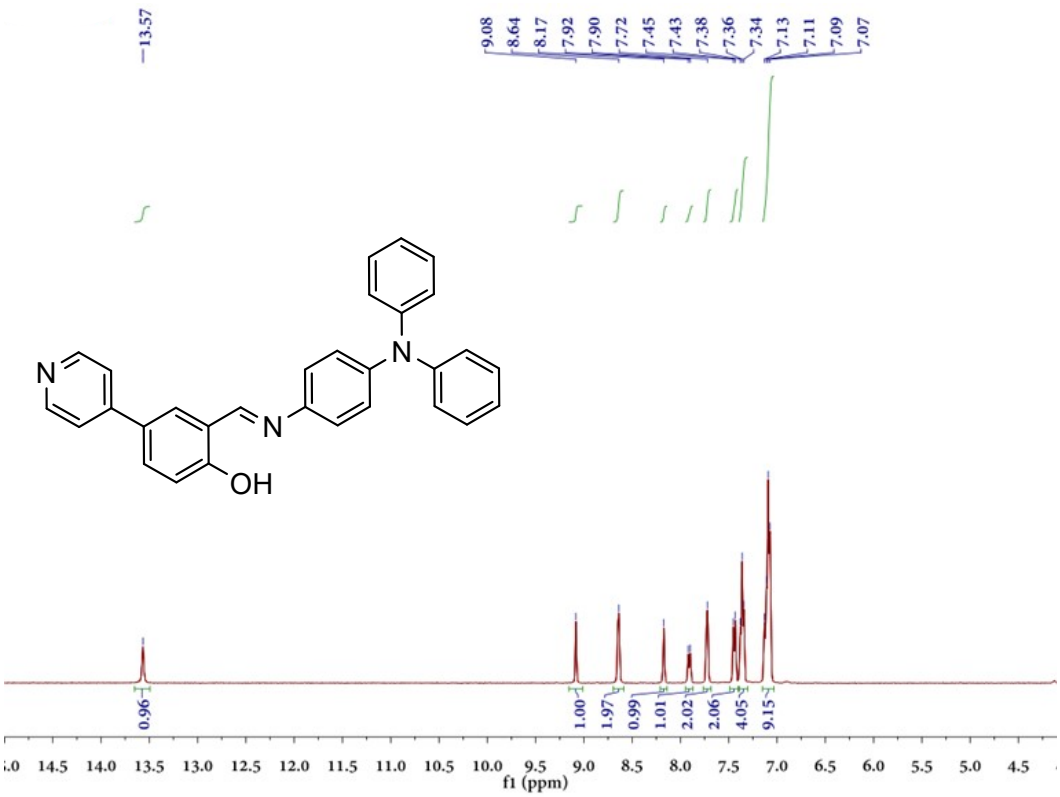

Fig. S3 ^{1}H NMR spectra of **HL** in DMSO-d_6.

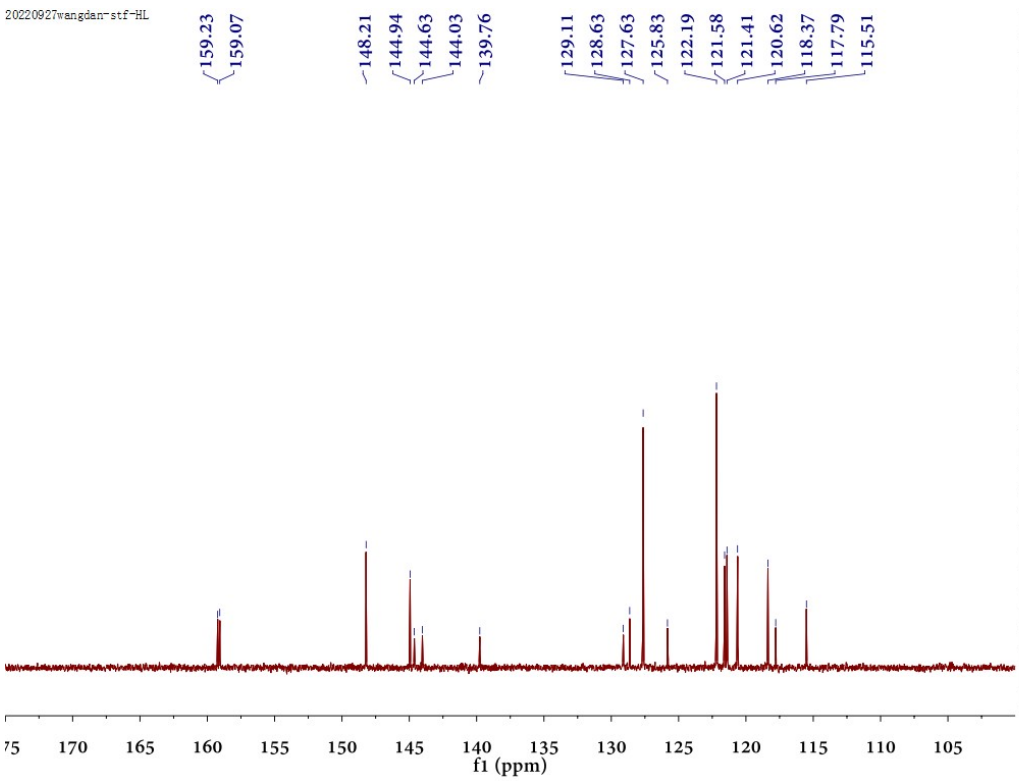

Fig. S4 ^{13}C NMR spectra of **HL** in DMSO-d_6.

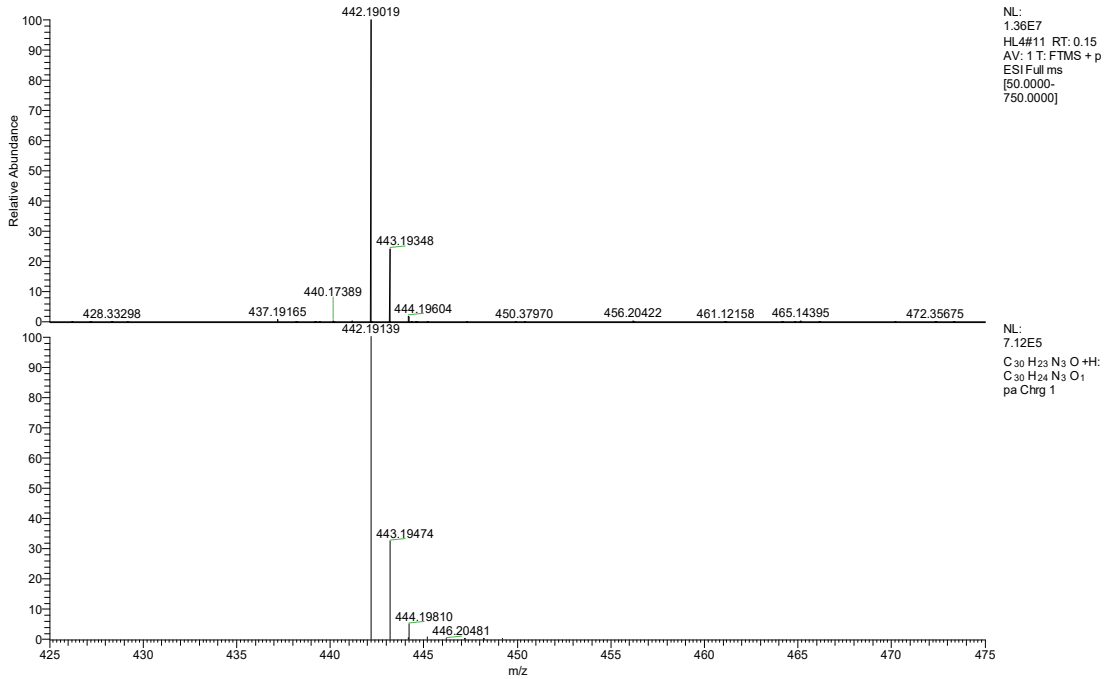

Fig. S5 (a) ESI-mass spectrum of **HL** ($C_{30}H_{23}N_3O$). (b) The simulation pattern of $[H(C_{30}H_{23}N_3O)]^+$.

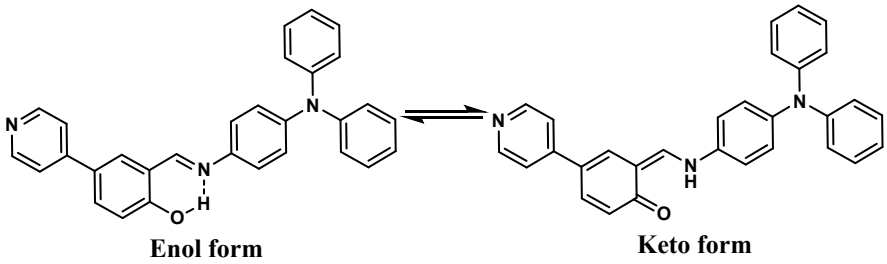

Scheme S2 The ESIPT process in **HL**.

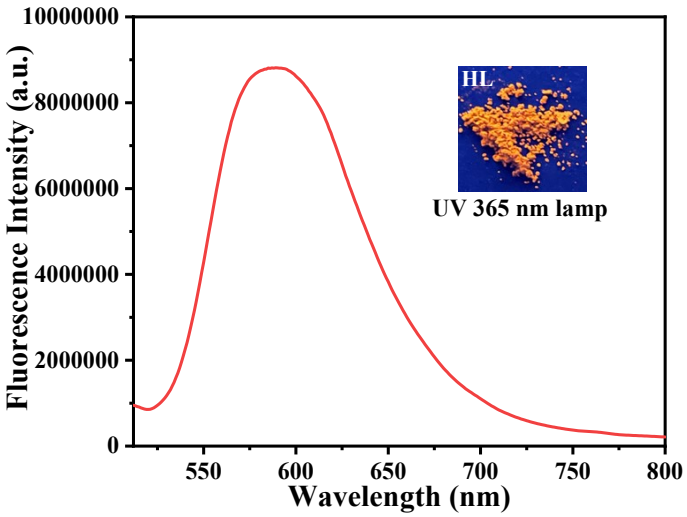

Fig. S6 Fluorescence emission spectrum of **HL** in the solid state, λ_{ex} = 465 nm. Inset: Fluorescence photograph of **HL** in the solid state under 365 nm UV lamp.

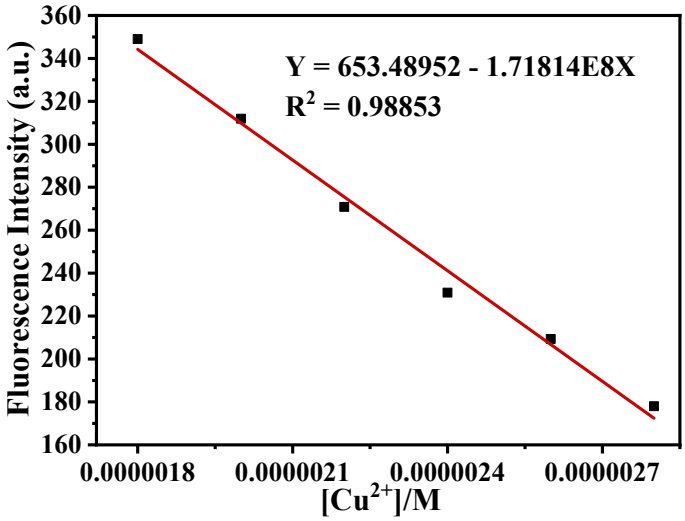

Fig. S7 Determination of detection limit of **HL** for Cu^{2+} by fluorescence titration experiment.

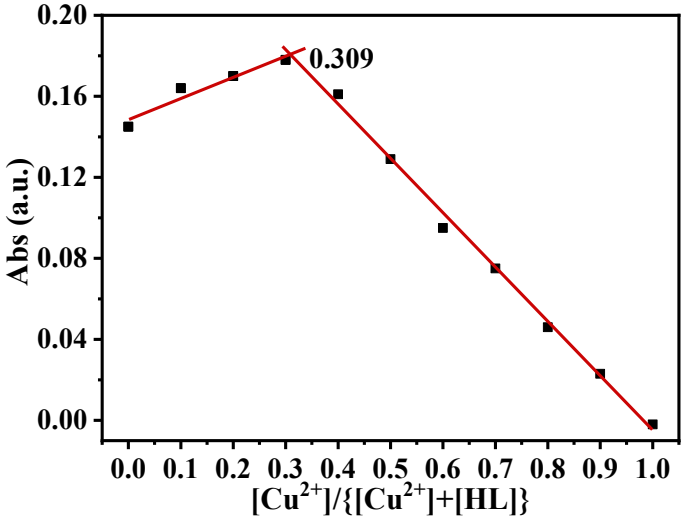

Fig. S8 Job's plot of Cu^{2+} vs **HL** in THF/H_2O (1/9, v/v) based on the absorbance at 343 nm.

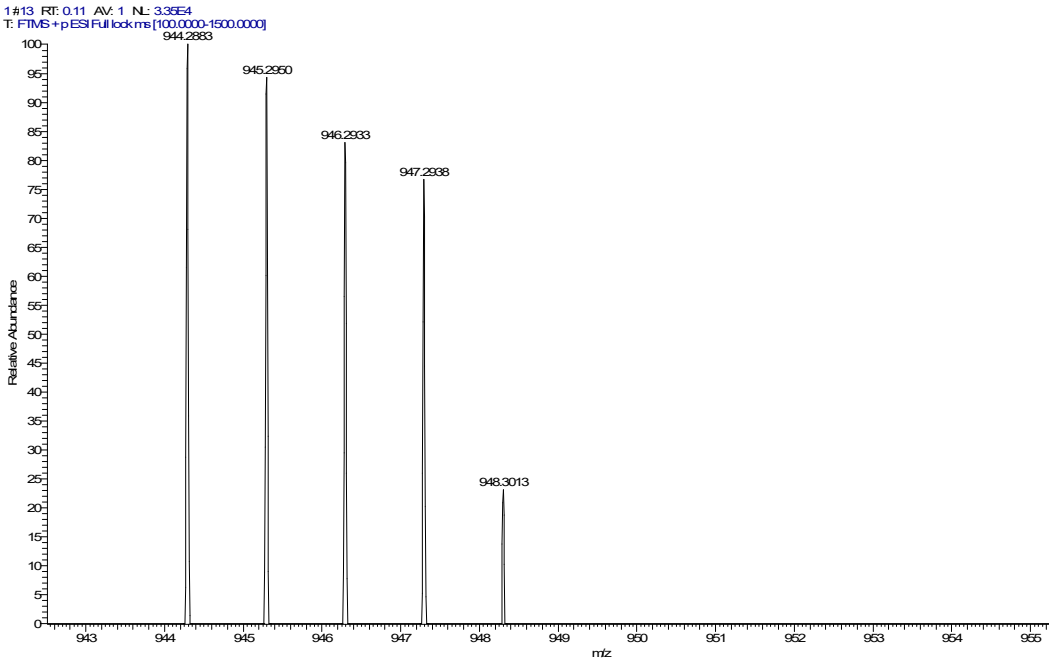

Fig. S9 ESI-HRMS of **HL** upon the addition of 0.5 equiv. Cu^{2+} in THF.

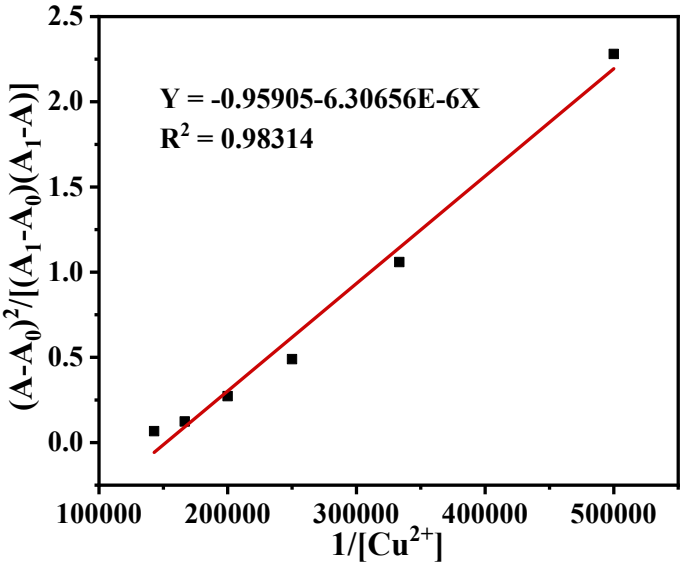

Fig. S10 Association constant calculations by plotting $(A-A_0)^2/[(A_1-A_0)(A_1-A)]$ vs $1/[Cu^{2+}]$ with linear fitting as well to find out the binding constant of $\mathbf{CuL_2}$, where A = absorbance at 343 nm at any given concentration of Cu^{2+}, A_0 = absorbance maxima at 343 nm in presence of Cu^{2+}, and A_1 = absorbance maxima at 343 nm in the absence of Cu^{2+}.

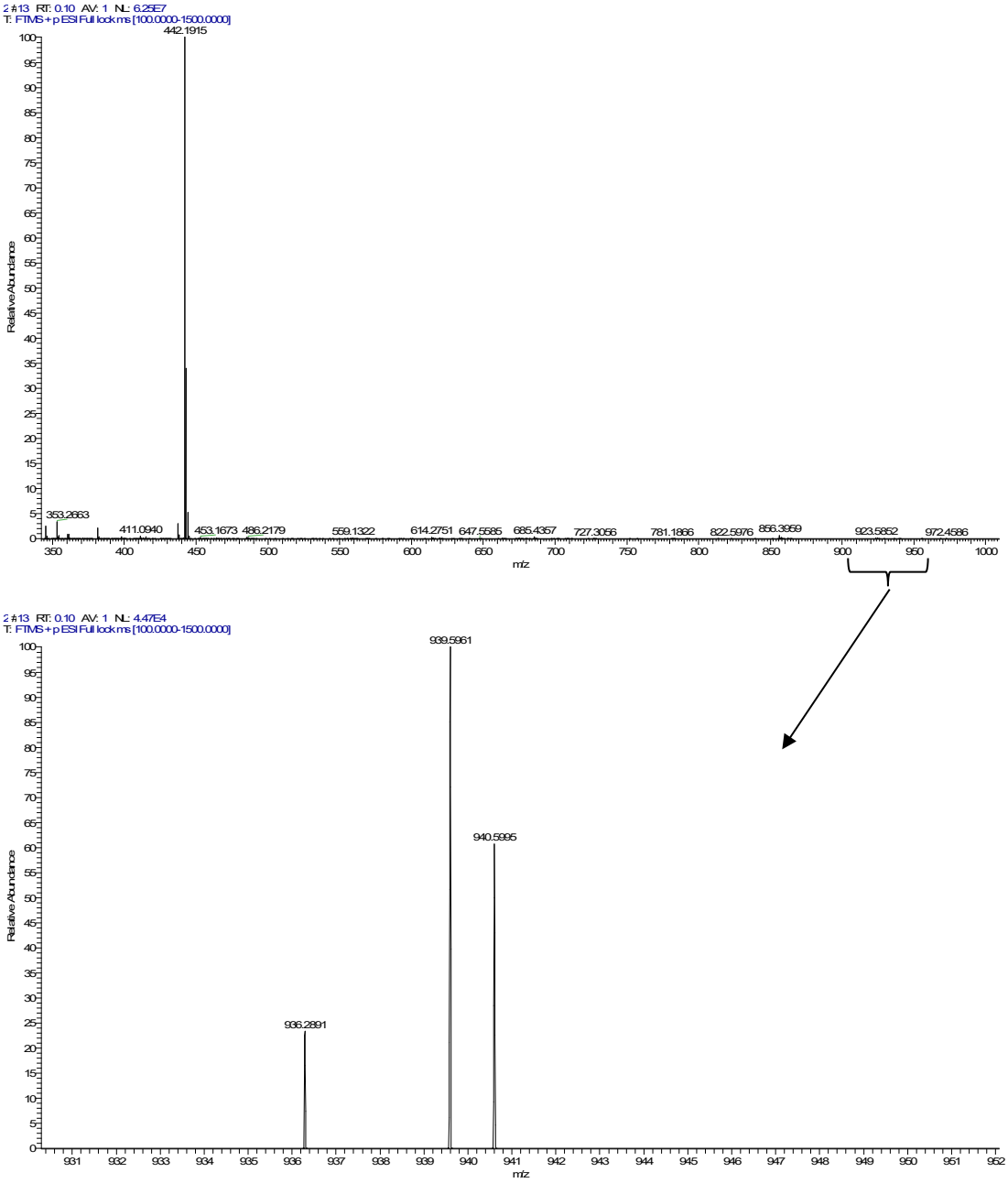

Fig. S11 ESI-HRMS of **CuL$_2$** upon the addition of 8.0 equiv. His in THF.

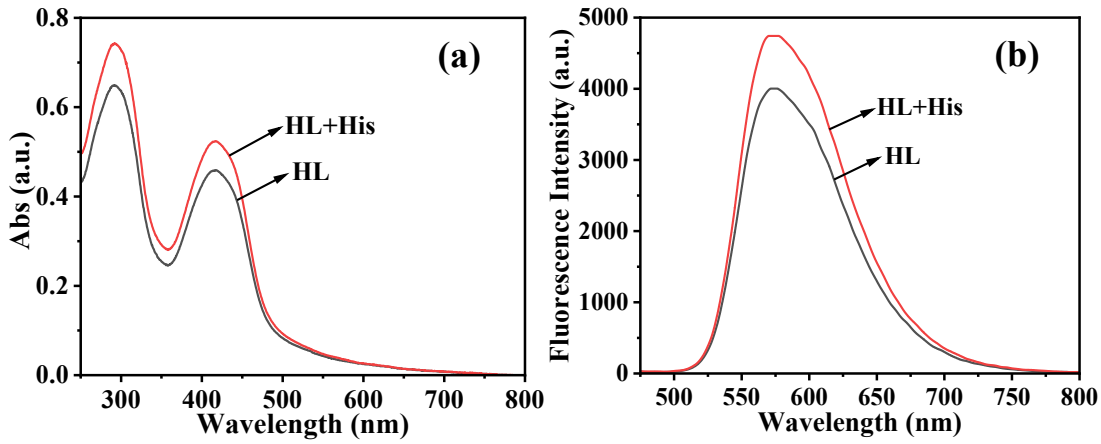

Fig. S12 UV-Vis (a) and fluorescence (b) spectra of **HL** (20 μM) and **HL** (20 μM)+4.0 equiv. His in THF/H_2O (1:9, v/v).

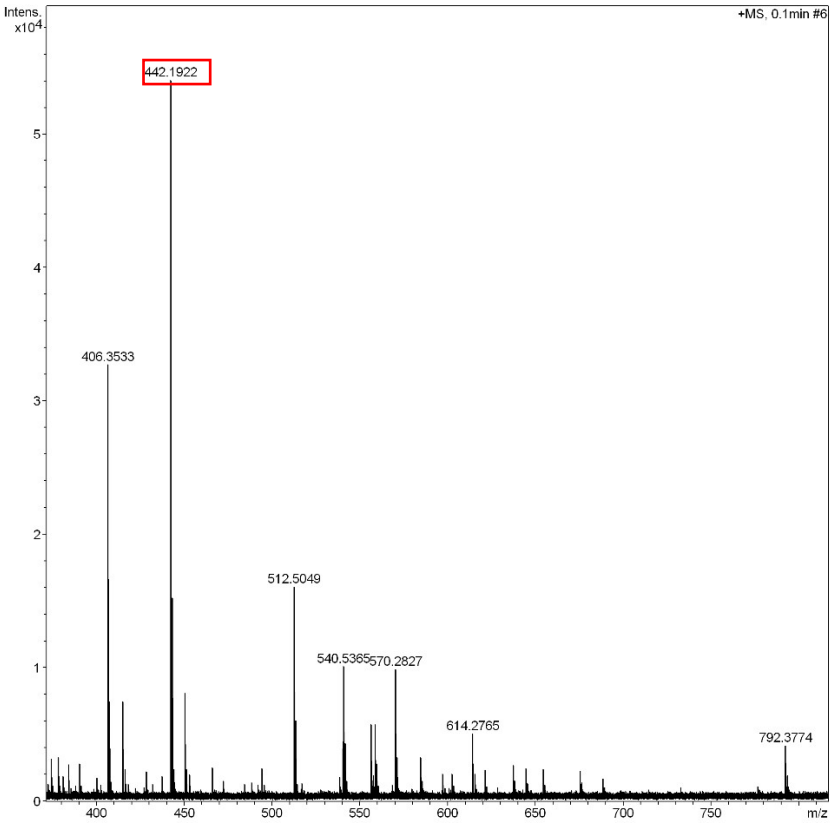

Fig. S13 ESI-HRMS of **HL**+His in THF/H_2O.

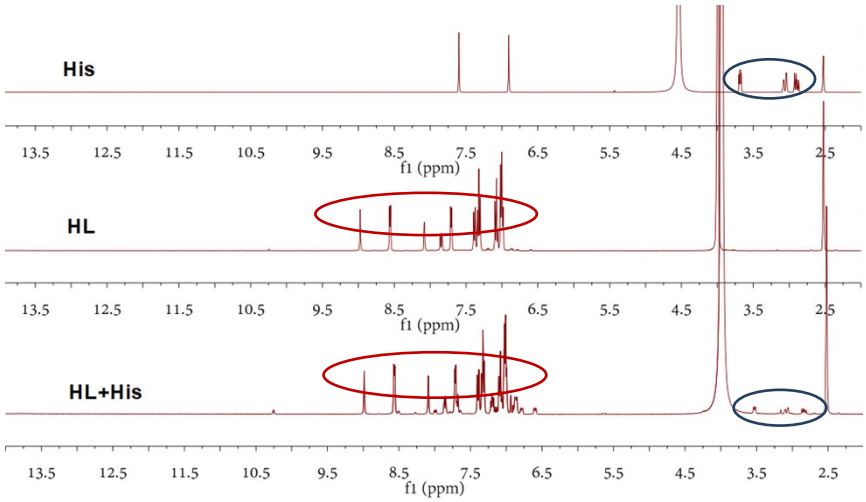

Fig. S14 ^{1}H NMR spectra of **HL**, His and **HL**+His in DMSO-d_6/D_2O.

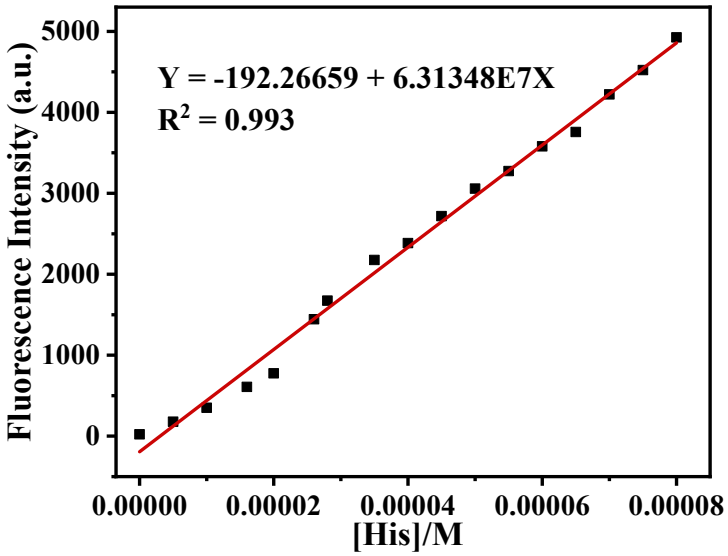

Fig. S15 Determination of detection limit of **CuL_2** for His by fluorescence titration experiment.

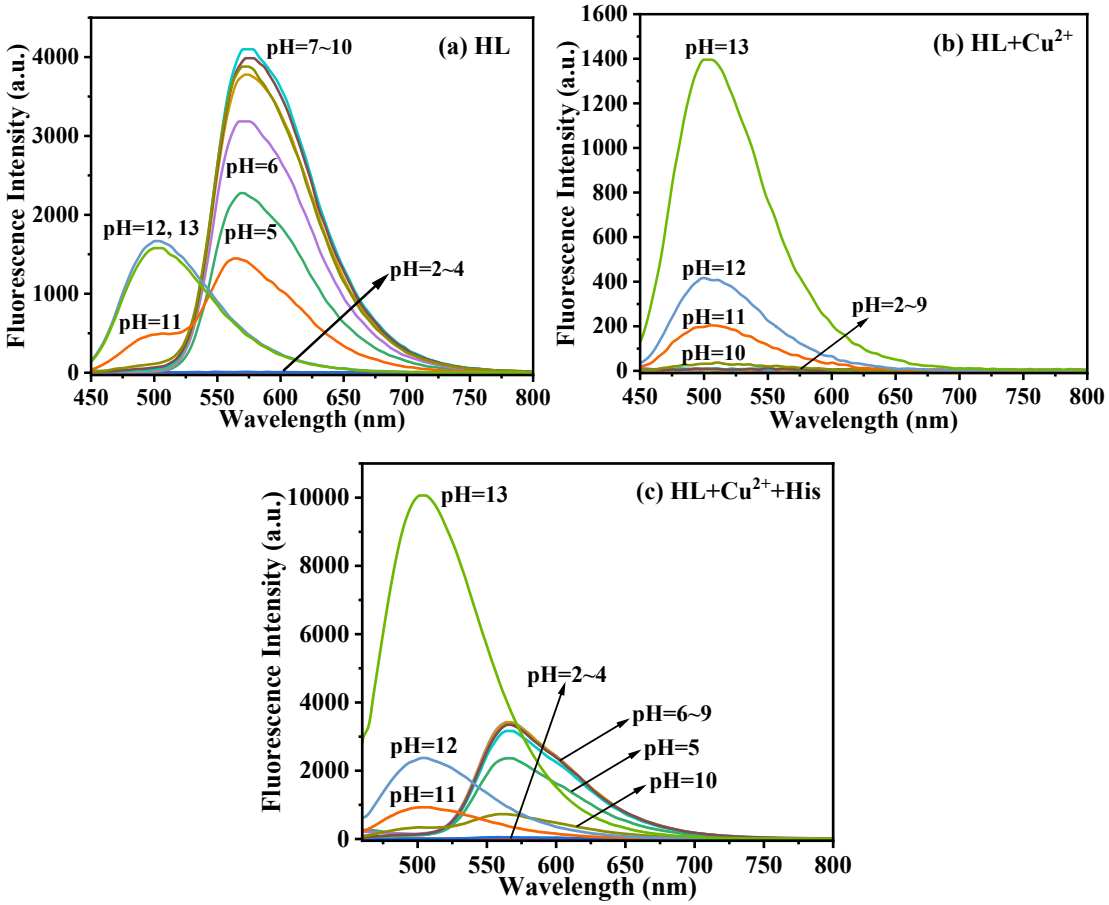

Fig. S16 Fluorescence spectra of **HL** (a), **HL**+Cu^{2+} (b) and **HL**+Cu^{2+}+His (c) in THF/H_2O (1:9, v/v) with different pH values, λ_{ex}= 420 nm.

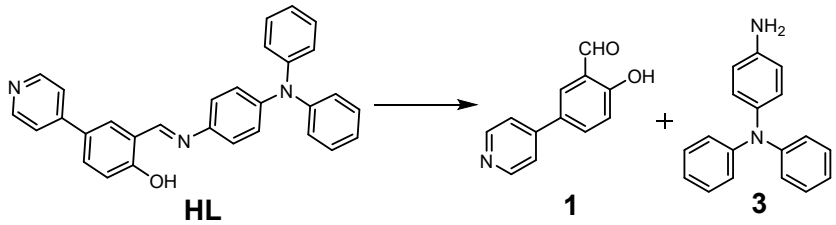

Scheme S3 The possible hydrolysis of **HL**.

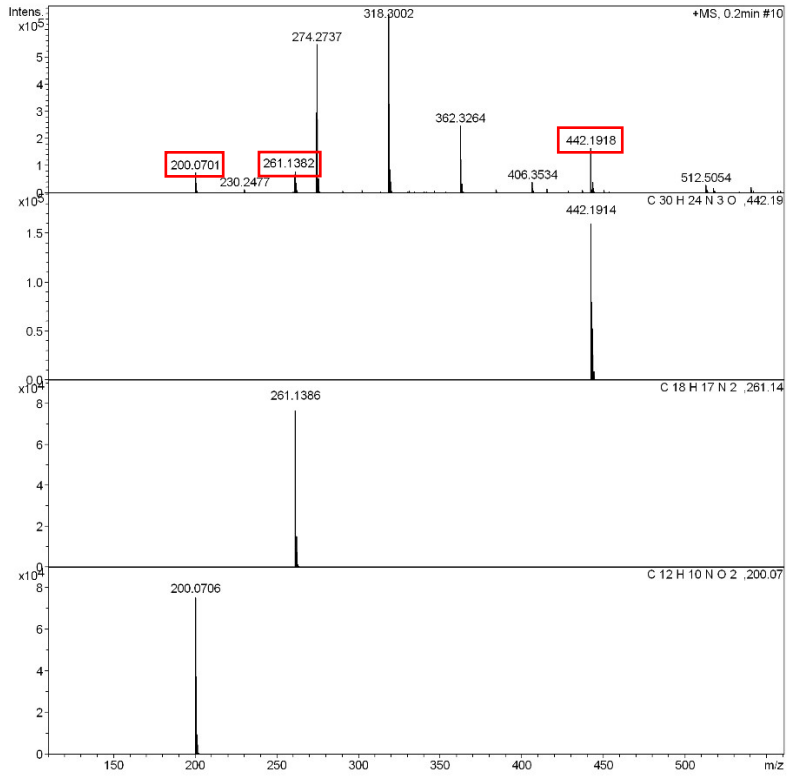

(a)

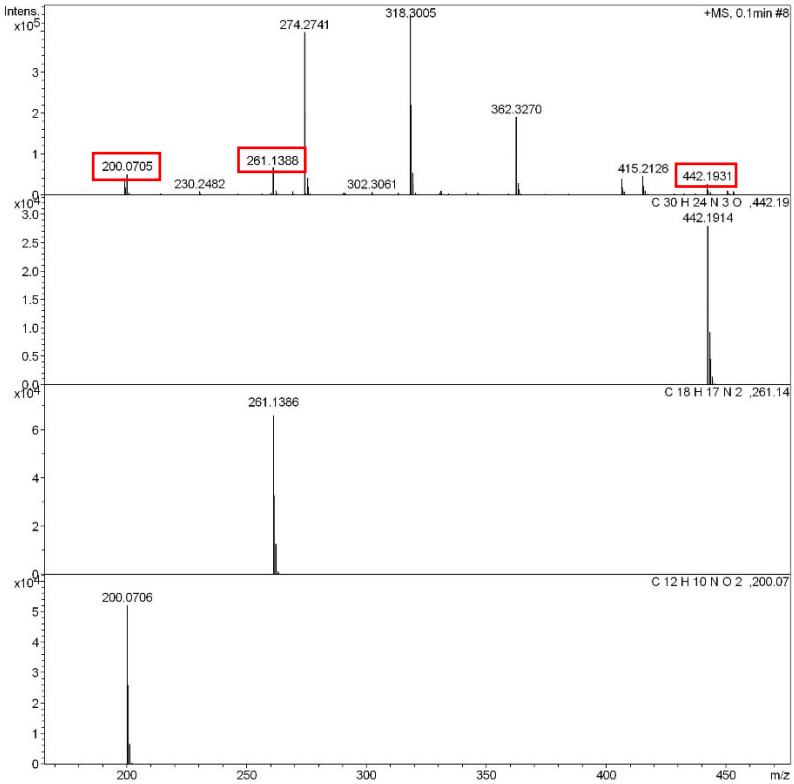

(b)

Fig. S17 ESI-HRMS of **HL** in THF/H_2O with pH values of 10 (a) and 13 (b).

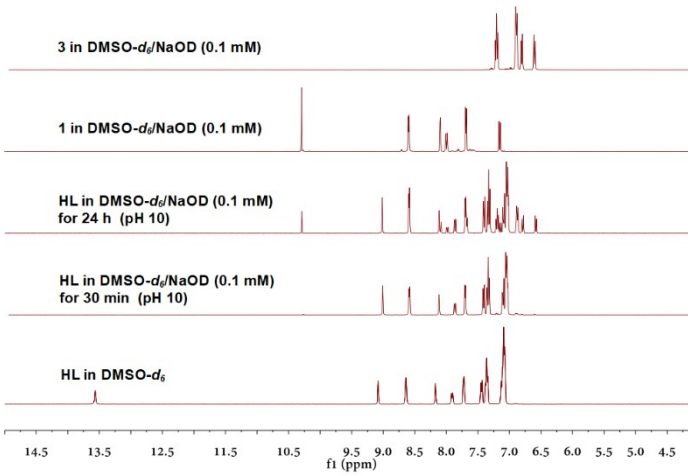

(a)

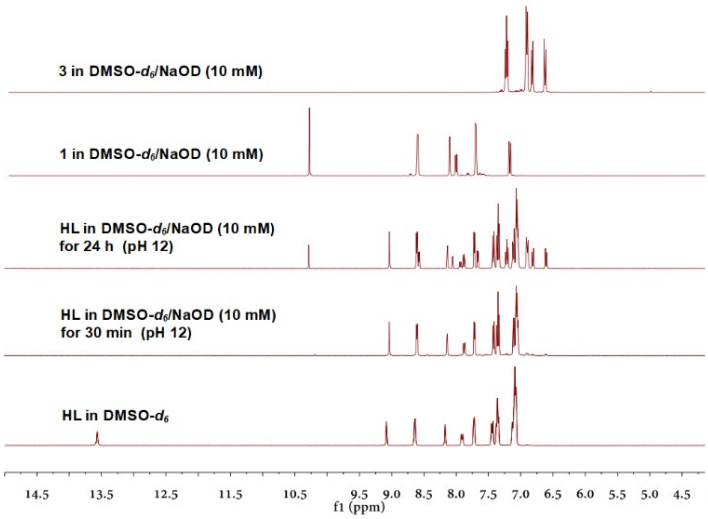

(b)

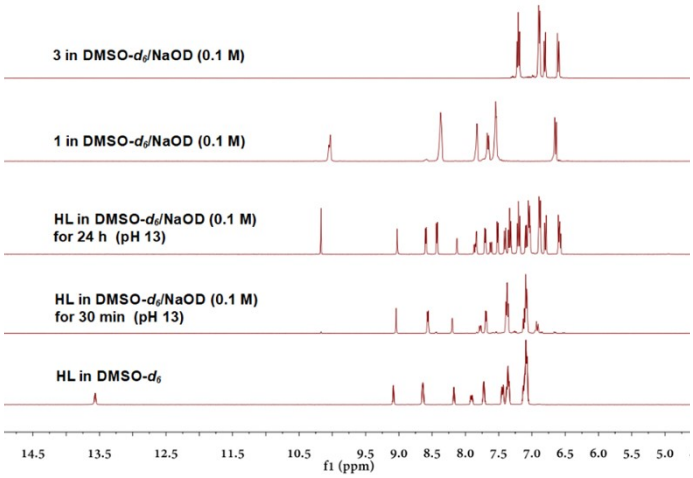

(c)

Fig. S18 ^{1}H NMR of **HL** in DMSO-d_6/D_2O with NaOD concentrations of 0.1 mM (pH 10) (a), 10 mM (pH 12) (b) and 0.1 M (pH 13) (c).

Table S1 Performance of **HL** compared with recent reported fluorescence probes for Cu^{2+} and His.

Refs.	Probe	Analyte	Response Mode	Detection Media	Emission Wavelength	Detection Limit	Test Strips	Cell Imaging	pH
13	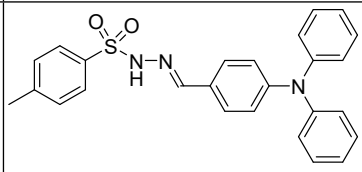	Cu^{2+}	Turn-off	ACN/H_2O, (7:3, v/v), pH=7.00	495 nm	1.25×10^{-8} M	—	—	3-8
14	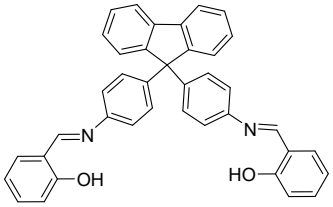	Cu^{2+}	Ratiometric	DMF/H_2O, (2:8, v/v)	318 nm	2.13×10^{-9} M	Yes	—	4-10
15	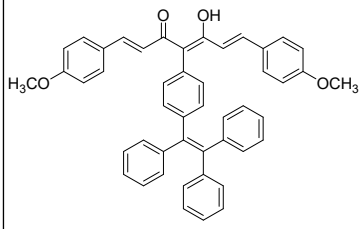	Cu^{2+}	on-off	H_2O/THF (4:1, v/v)	525 nm	1.49×10^{-7} M	Yes	—	5-10
16	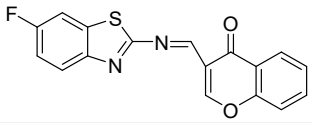	Cu^{2+}	colorimetric	THF /EtOH	428 nm	0.273×10^{-6} M	—	Yes	—
17	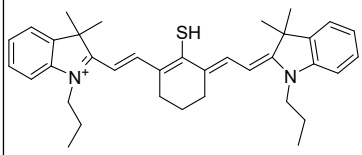	Cu^{2+}	turn-on	HEPES/EtOH, (v/v = 1/1), pH=7.4,	784 nm	1.24×10^{-7} M	—	Yes	4-9
18	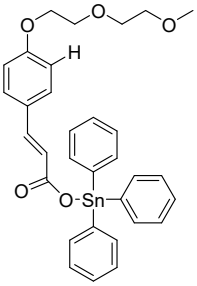	Cu^{2+}	on-off	DMSO	360 nm	—	—	Yes	—
19	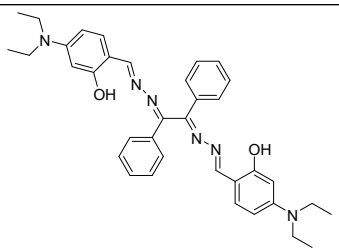	Cu^{2+}	on-off	THF/H_2O (1:1, v/v)	598 nm	2×10^{-7} M	Yes	—	—

20	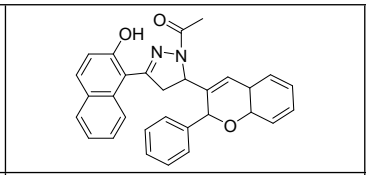	Cu^{2+}	on-off	EtOH/H_2O (1:1, v/v), (HEPES=10 mM, pH=7.4)	417 nm	8.85×10^{-7} M	—	Yes	7.4
21	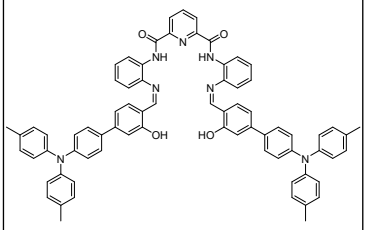	Cu^{2+}	on-off	THF/H_2O (4:1, v/v),2.00 × 10^{-3} M Tris-HCl buffer, pH=7.00)	598 nm	2.687×10^{-7} M	—	—	3-11
22	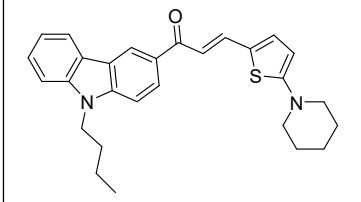	Cu^{2+}	on-off	HEPES/CH_3CN (0.5:9.5, v/v, 10 mM HEPES buffer, pH=7.4)	546 nm	2.9×10^{-10} M	—	Yes	4-8
23	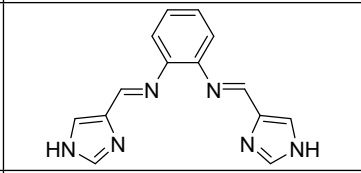	Cu^{2+}	on-off	H_2O	402 nm	2.7×10^{-9} M	—	Yes	4.85-11.24
24	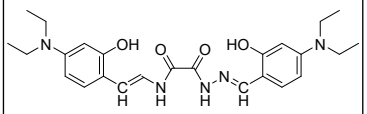	Cu^{2+}	colorimetric	DMSO/H_2O (7:3, v/v), 5 mM NaAc–HAc , pH=7.0	520 nm	1.2×10^{-7} M	—	—	
25	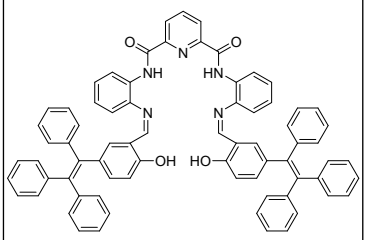	Cu^{2+}	on-off	THF/H_2O (4:1, v/v), pH = 7.0	598 nm	2.36×10^{-7} M	—	—	2-11
26	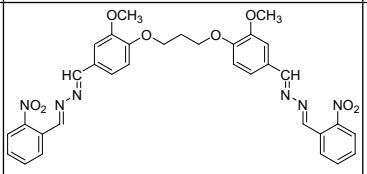	Cu^{2+}, His	on-off-on	DMSO/H_2O (1:1, v/v)	410 nm	$14-18 \times 10^{-7}$ M, $6-11 \times 10^{-7}$ M	—	—	6-7
27	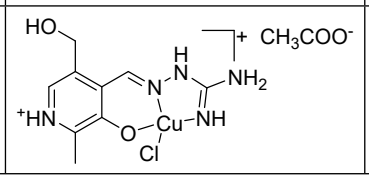	His	colorimetric	H_2O (0.01 M HEPES buffer, pH=7.4)	443 nm	8.5×10^{-8} M, 1.9×10^{-7} M	—	—	—

	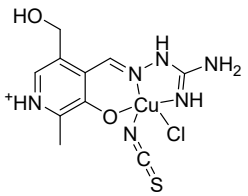								
28	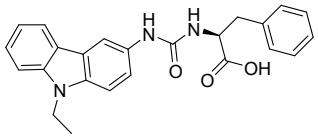	His	on-off-on	H_2O /acetonitrile (99:1, v/v)	395 nm	7.64×10^{-6} M	—	—	—
29	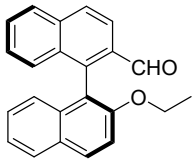	His	off-on	^{i}PrOH /MeOH (99/1, v/v)	365 nm	7.03×10^{-8} M	—	—	—
30	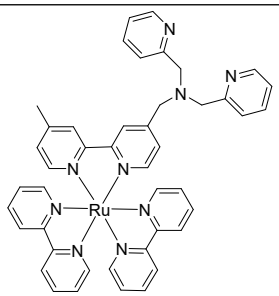	Cu^{2+}, His	on-off-on	HEPES buffer (10 mM, pH=7.4)	610 nm	0.04×10^{-6} M, 1.4×10^{-6} M	—	Yes	2-12
31	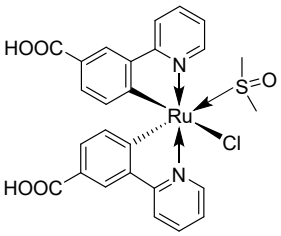	His	off-on	DMSO, 0.01 M PB (pH=7.4)	473 nm	1×10^{-7} M	—	—	—
32	Cu-MOFs/Fe^{3+}	His	turn-on	H_2O	430 nm	1.56×10^{-7} M	—	—	—
33	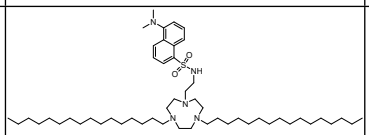	Cu^{2+}, His	on-off-on	DOPC	513 nm	2.4×10^{-8} M, 5.4×10^{-8} M	Yes	—	—
This work	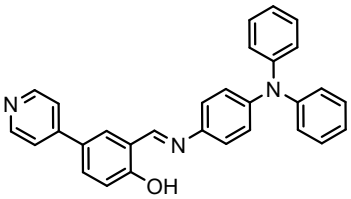	Cu^{2+}, His	on-off-on	THF/H_2O (1:9, v/v)	560 nm	1.32×10^{-7} M, 5.14×10^{-8} M	Yes	Yes	5-10, 5-9

Table S2 Crystal data and structure refinement for **HL** and **ZnL_2**.

Identification code	**HL**	**ZnL_2**
Empirical formula	$C_{30}H_{23}N_3O$	$C_{60}H_{44}N_6O_2Zn$
Formula weight	441.51	946.38
Crystal system	Monoclinic	Triclinic

Space group	$P2_1/n$	$P\bar{1}$
a/Å	15.6216(9)	11.9862(10)
b/Å	9.9838(5)	14.4619(13)
c/Å	16.1858(9)	15.5093(13)
α/°	90	85.024(2)
β/°	113.984(2)	72.211(2)
γ/°	90	74.526(2)
Volume/Å^3	2306.4(2)	2467.1(4)
Z	4	2
ρ_{calc}g/cm^3	1.271	1.274
μ/mm^{-1}	0.078	0.548
F(000)	928.0	984.0
Index ranges	$-18 \leq h \leq 20$, $-13 \leq k \leq 13$, $-21 \leq l \leq 21$	$-14 \leq h \leq 9$, $-17 \leq k \leq 17$, $-18 \leq l \leq 18$
Reflections collected	22181	18149
Independent reflections	5607 [R_{int} = 0.0453, R_{sigma} = 0.0404]	8416 [R_{int} = 0.0352, R_{sigma} = 0.0473]
Data/restraints/parameters	5607/0/308	8416/87/677
Goodness-of-fit on F^2	1.045	1.055
Final R indexes [I>=2σ (I)]	R_1 = 0.0613, wR_2 = 0.1613	R_1 = 0.0482, wR_2 = 0.1218
Final R indexes [all data]	R_1 = 0.0899, wR_2 = 0.1809	R_1 = 0.0615, wR_2 = 0.1339
Largest diff. peak/hole / e Å^{-3}	0.21/-0.14	0.49/-0.37
CCDC number	2211845	2211846

$R_1 = \Sigma(|F_o| - |F_c|)/|F_o|$; $wR_2 = \{\Sigma[(w|F^2_o| - |F^2_c|)^2/\Sigma w(F^2_o)^2]\}^{1/2}$.

Table S3 Selected bond distances (Å) and angles (deg) for **HL** and **ZnL_2**.

HL			
O1-C21	1.343(2)	C26-C30	1.383(2)
N1-C19	1.275(2)	C26-C27	1.383(3)
N1-C16	1.4177(19)	C12-C11	1.374(3)
N2-C13	1.433(2)	C12-C7	1.380(3)
N2-C6	1.398(2)	C21-C22	1.395(2)
N2-C12	1.417(2)	C16-C17	1.372(2)
C20-C25	1.386(2)	C16-C15	1.389(3)
C20-C19	1.456(2)	C18-C17	1.385(2)
C20-C21	1.401(2)	C11-C10	1.370(3)
C24-C25	1.390(2)	C14-C15	1.383(2)
C24-C26	1.478(2)	C23-C22	1.368(3)
C24-C23	1.391(2)	C2-C3	1.379(3)
C13-C18	1.373(3)	C3-C4	1.357(3)
C13-C14	1.374(3)	C5-C4	1.373(3)
N3-C29	1.323(3)	C10-C9	1.364(4)
N3-C28	1.321(3)	C7-C8	1.378(3)

C6-C1	1.379(3)	C30-C29	1.376(3)
C6-C5	1.394(2)	C27-C28	1.374(3)
C1-C2	1.377(3)	C9-C8	1.363(4)
C19-N1-C16	121.95(15)	O1-C21-C20	121.95(15)
C6-N2-C13	120.09(14)	O1-C21-C22	119.57(17)
C6-N2-C12	122.44(14)	C22-C21-C20	118.48(17)
C12-N2-C13	117.39(14)	C17-C16-N1	116.64(15)
C25-C20-C19	119.17(15)	C17-C16-C15	118.33(15)
C25-C20-C21	119.24(15)	C15-C16-N1	125.03(16)
C21-C20-C19	121.59(16)	C13-C18-C17	120.48(18)
C25-C24-C26	120.93(15)	C10-C11-C12	120.8(2)
C25-C24-C23	116.83(16)	C13-C14-C15	120.62(18)
C23-C24-C26	122.23(14)	C16-C17-C18	120.98(17)
C18-C13-N2	120.18(17)	C22-C23-C24	121.96(15)
C18-C13-C14	119.03(16)	C14-C15-C16	120.52(18)
C14-C13-N2	120.77(17)	C1-C2-C3	120.6(2)
C28-N3-C29	114.68(19)	C4-C3-C2	119.1(2)
C1-C6-N2	120.83(16)	C4-C5-C6	120.6(2)
C1-C6-C5	117.98(17)	C3-C4-C5	121.1(2)
C5-C6-N2	121.19(17)	C9-C10-C11	120.3(2)
C2-C1-C6	120.68(19)	C8-C7-C12	119.4(2)
C20-C25-C24	122.63(16)	C23-C22-C21	120.85(17)
C30-C26-C24	123.40(16)	C29-C30-C26	120.1(2)
C30-C26-C27	114.91(18)	C28-C27-C26	120.56(19)
C27-C26-C24	121.69(15)	C8-C9-C10	119.1(2)
C11-C12-N2	119.48(18)	N3-C29-C30	125.0(2)
C11-C12-C7	118.88(19)	N3-C28-C27	124.6(2)
C7-C12-N2	121.64(18)	C9-C8-C7	121.3(2)
N1-C19-C20	122.00(16)		
		ZnL_2	
N1-Zn1	2.007(2)	O1-Zn1	1.919(2)
N4-Zn1	2.018(2)	O2-Zn1	1.920(2)
C16-N1-Zn1	121.97(19)	C19-N1-Zn1	119.1(2)
C46-N4-Zn1	121.46(19)	C49-N4-Zn1	119.4(2)
C25-O1-Zn1	124.9(2)	C51-O2-Zn1	124.77(19)
N1-Zn1-N4	125.33(10)	O1-Zn1-N1	97.47(10)
O1-Zn1-N4	109.34(10)	O1-Zn1-O2	116.57(10)
O2-Zn1-N1	112.68(9)	O2-Zn1-N4	96.75(9)

References

1. S. J. Yeh, C. Y. Tsai, C.-Y. Huang, G.-S. Liou and S.-H. Cheng, *Electrochem. Commun.*, 2003, **5**,

373-377.
2. H. Tan, H. Yu, H. Yao, Y. Song, S. Zhu, N. Song, K. Shi, B. Zhang and S. Guan, *Dyes Pigm.*, 2018, **151**, 179-186.
3. M. J. Frisch, G. W. Trucks, H. B. Schlegel, G. E. Scuseria, M. A. Robb, J. R. Cheeseman, G. Scalmani, V. Barone, B. Mennucci, G. A. Petersson, H. Nakatsuji, M. Caricato, X. Li, H. P. Hratchian, A. F. Izmaylov, J. Bloino, G. Zheng, J. L. Sonnenberg, M. Hada, M. Ehara, K. Toyota, R. Fukuda, J. Hasegawa, M. Ishida, T. Nakajima, Y. Honda, O. Kitao, H. Nakai, T. Vreven, J. A. Montgomery Jr., J. E. Peralta, F. Ogliaro, M. Bearpark, J. J. Heyd, E. Brothers, K. N. Kudin, V. N. Staroverov, R. Kobayashi, J. Normand, K. Raghavachari, A. Rendell, J. C. Burant, S. S. Iyengar, J. Tomasi, M. Cossi, N. Rega, J. M. Millam, M. Klene, J. E. Knox, J. B. Cross, V. Bakken, C. Adamo, J. Jaramillo, R. Gomperts, R. E. Stratmann, O. Yazyev, A. J. Austin, R. Cammi, C. Pomelli, J. W. Ochterski, R. L. Martin, K. Morokuma, V. G. Zakrzewski, G. A. Voth, P. Salvador, J. J. Dannenberg, S. Dapprich, A. D. Daniels, O. Farkas, J. B. Foresman, J. V. Ortiz, J. Cioslowski and D. J. Fox, *Journal*, 2009.
4. C. Adamo and V. Barone, *J. Chem. Phys.*, 1999, **110**, 6158-6170.
5. F. Weigend and R. Ahlrichs, *Phys. Chem. Chem. Phys.*, 2005, **7**, 3297-3305.
6. F. Weigend, *Phys. Chem. Chem. Phys.*, 2006, **8**, 1057-1065.
7. S. Grimme, S. Ehrlich and L. Goerigk, *J. Comput. Chem.*, 2011, **32**, 1456-1465.
8. A. V. Marenich, C. J. Cramer and D. G. Truhlar, *J. Phys. Chem. B*, 2009, **113**, 6378-6396.
9. T. Lu and F. Chen, *J. Comput. Chem.*, 2012, **33**, 580-592.
10. W. Humphrey, A. Dalke and K. Schulten, *J. Mol. Graphics*, 1996, **14**, 33-38.
11. A. Schaefer, H. Horn and R. Ahlrichs, *J. Chem. Phys.*, 1992, **97**, 2571-2577.
12. A. Schaefer, C. Huber and R. Ahlrichs, *J. Chem. Phys.*, 1994, **100**, 5829-5835.
13. D. Mohanasundaram, R. Bhaskar, N. Lenin, K. Nehru, G. Rajagopal, G. G. V. Kumar and J. Rajesh, *Journal of Photochemistry and Photobiology A: Chemistry*, 2022, **427**, 113850.
14. S. Majeed, T. A. Khan, M. T. Waseem, H. M. Junaid, A. M. Khan and S. A. Shahzad, *Journal of Photochemistry and Photobiology A: Chemistry*, 2022, **431**, 114062.
15. Y. Lin, A. Yu, J. Wang, D. Kong, H. Liu, J. Li and C. Jia, *RSC Advances*, 2022, **12**, 16772-16778.
16. R. Kouser, A. Rehman, S. M. A. Abidi, F. Arjmand and S. Tabassum, *Journal of Molecular Structure*, 2022, **1256**, 132533.
17. T. Guo, R. Tian, W. Qu, B. Yang, Z. Geng and Z. Wang, *Dyes and Pigments*, 2022, **205**, 110483.
18. Z. Fang, D. Chen, J. Xu, S. Liu, G. Xu, X. Tian, J. Xuan, Y. Tian and Q. Zhang, *Sensors and Actuators B: Chemical*, 2022, **357**, 131423.
19. M. Zhu, S. Huang, M. Chen, Y. Li and M. Zhong, *Optical Materials*, 2022, **127**, 112288.
20. Y.-p. Zhang, Y.-c. Zhao, Q.-h. Xue, Y.-s. Yang, H.-C. Guo and J.-J. Xue, *Inorganic Chemistry Communications*, 2021, **129**, 108612.
21. X. Zhang, S.-T. Wu, X.-J. Yang, L.-Y. Shen, Y.-L. Huang, H. Xu, Q.-L. Zhang, T. Sun, C. Redshaw and X. Feng, *Inorg. Chem.*, 2021, **60**, 8581-8591.
22. H. Wang, P. Wang, L. Niu, C. Liu, Y. Xiao, Y. Tang and Y. Chen, *Spectrochimica Acta Part A: Molecular and Biomolecular Spectroscopy*, 2022, **278**, 121257.
23. H.-j. Yu, W. Zhao, Y. Zhou, G.-j. Cheng, M. Sun, L. Wang, L. Yu, S. H. Liang and C. Ran, *Analytica Chimica Acta*, 2020, **1097**, 144-152.
24. B. Wang, W. Xu, K. Gan, K. Xu, Q. Chen, W. Wei and W. Wu, *Spectrochimica Acta Part A: Molecular and Biomolecular Spectroscopy*, 2022, **277**, 121245.

25. H.-F. Xie, C.-J. Yu, Y.-L. Huang, H. Xu, Q.-L. Zhang, X.-H. Sun, X. Feng and C. Redshaw, *Mater. Chem. Front.*, 2020, **4**, 1500-1506.
26. B. Mohan, K. Modi, J. Parikh, S. Ma, S. Kumar, K. Kumar Manar, F. Sun, H. You and P. Ren, *Journal of Photochemistry and Photobiology A: Chemistry*, 2022, **422**, 113557.
27. M. Chakraborty, M. Mohanty, R. Dinda, S. Sengupta and S. Kumar Chattopadhyay, *Polyhedron*, 2022, **211**, 115554.
28. A. Pundi, C.-J. Chang, J. Chen, S.-R. Hsieh and M.-C. Lee, *Sens. Actuators, B*, 2021, **328**, 129084.
29. J. Tian, K. Lu, Y. Wang, Y. Chen, B. Huo, Y. Jiang, S. Yu, X. Yu and L. Pu, *Tetrahedron*, 2021, **95**, 132366.
30. Y. Yang, Y. Li, X. Zhi, Y. Xu and M. Li, *Dyes Pigm.*, 2020, **183**, 108690.
31. M. Zhang, M. Qian, H. Huang, Q. Gao, C. Zhang and H. Qi, *Journal of Electroanalytical Chemistry*, 2022, **920**, 116578.
32. C. Chu, R. Huang, X. Wang, Y. Deng, T. Gu, D. Huo, L. Zhang, D. Zhong and C. Hou, *Nano*, 2020, **16**, 2150015.
33. B. Maiti, N. Dey and S. Bhattacharya, *ACS Applied Bio Materials*, 2019, **2**, 2365-2373.